Volume-6 | Issue-12 | December-2017 | ISSN No 2277 - 8179 | IF : 4.176 | IC Value : 93.98

INTERNATIONAL JOURNAL OF SCIENTIFIC RESEARCH

INTERMETALLIC COMPOUND FORMATION AT THE INTERFACE OF THE DIFFUSION BONDED JOINTS TI-4.5AL-2MO-1.8V-0.5FE AND AISI 410 STAINLESS STEEL

Engineering

Dr.T.Vigraman* Associate Professor S.G, Department of Mechanical Engineering, National Engineering College, K.R.Nagar, Kovilpatti, Tamilnadu, India. *Corresponding Author

ABSTRACT

The present study discusses the formation of interfacial reaction products in the dissimilar diffusion bonded joints made between AISI 410 and Ti-4.5Al-2Mo-1.8V-0.5 Fe (Ti-alloy). Diffusion bonding was carried out in the temperature range of 800 -900°C with an interval of 50 °C, holding time 45min and a pressure of 8 MPa. A maximum shear strength of 64.2 MPa was obtained for the diffusion bonded joints processed at a temperature 850°C, holding time 45min and 8 MPa pressure. Optical and SEM images revealed a distinct diffused region rich with intermetallic compounds at the interface. The EDAX and XRD performed at the interface corroborated the presence of intermetallic compounds and carbides such as Fe_2Ti, Ti_2Al, $FeAl_2$, Fe_3MoSi, TiAl, TiFe, $MoSi_2$, FeCrAl, CrC, VC and, TiC.

KEYWORDS

Diffusion bonding, Ti-alloy, martensitic stainless steel, intermetallic compounds, fractograph.

1. INTRODUCTION

In general titanium and titanium alloys possess good mechanical properties and corrosion and high temperature properties. The Ti-alloy Ti-4.5Al-2Mo-1.8V-0.5 Fe is a dual phase alloy containing alpha and beta phase. The alpha stabilizing element aluminium and beta stabilizing elements such as vanadium, molybdenum and iron are present in this alloy. Martensitic stainless steel possess good strength, high temperature and wear resistant properties. The corrosion resistant properties are better than ferritic stainless steels, but inferior to austenitic stainless steels. Sedat Kolukisa [1] presented martensitic stainless steels can be heat-treated, though it contains more than 11.5% chromium and austenite stabilizing elements such as carbon, nitrogen and nickel. Dissimilar metals cannot be fusion welded because of difference in co-efficient of thermal expansion, residual stresses built at the joint region and brittle intermetallic compounds formed during welding. Therefore, diffusion bonding is one of the solid state welding process suitable for joining dissimilar metals of entirely different species Vigraman et al [2].

He et al [3] reported the formation of Ti_3Al intermetallic compound and Ti solid solution at the interface between TiAl intermetallic compound and Ti interlayer, further, vanadium and copper interlayer's prevented the formation TiC and Fe-Ti-Al compounds at the interface between the steel and Ti-Cu interlayers. Kundu and Chatterjee [4] performed direct diffusion bonding of pure titanium with micro duplex stainless steel at 800-950 °C for a bonding time of 1.5 h and at a bonding pressure of 3MPa. The width of the interface was more for the samples processed at higher temperatures because of this the strength of the joints were less. Kundu and Chatterjee [5] conducted diffusion bonding between titanium and stainless steel with a nickel interlayer. Intermetallic compounds such as Ni3Ti, Ni_2Ti and NiTi were formed at the interface between titanium and nickel interlayer. Qin et al [6] performed vacuum diffusion bonding of titanium alloy with austenitic stainless steel under cyclic thermal loading conditions between 800-890 °C, at a pressure of 5 MPa and a heating rate of 30 °C /s. Kundu et al [7] reported diffusion bonded joints strength as 318 MPa at a bonding temperature of 900 °C for the joints made between pure titanium and austenitic stainless steel AISI 304 using copper interlayer. Ti-alloy Ti-4.5Al-2Mo-1.8V-0.5 Fe is selected as base metal to bond with AISI 410 to improve the corrosion resistant properties of AISI 410 steel. The control of process parameters like temperature, bonding pressure and bonding time is essential along with protective environment throughout the process to achieve sound bonding during DB process. The lateral deformations of the bonded samples are prevented using a specially designed fixture. Further, the surface asperities are broken by applying heavy impulse pressure on the diffusion bonded samples before raising the temperature in the furnace. The intermetallic compounds and secondary phases formed at the interface between the two base metals alter the electrical conductivity of the base metals. The objective of the study is to make the dissimilar joints and study the variation in the electrical properties of the joints under static loads and at elevated temperatures.

2. EXPERIMENTAL PROCEDURE

Diffusion bonding experiments were conducted in the temperature range of 800-900 °C with an interval of 50 °C, holding pressures set at 8 MPa and a bonding time of 45 min as shown in the Table 1. The Ti-alloy and AISI 410 were purchased in the form of 20 mm diameter rods. The chemical composition of the base metals Ti-alloy is 93%Ti, 4.58%Al, 2.1%Mo, 1.83%V, 0.54%Fe, , 0.12%Si, 0.014%C and AISI 410 steel is 0.12%C, 12.5%Cr. 0.28%Si, 0.48%Ni, 0.15%Cu, 0.24%Mn. They were cut into billets of 20 mm in height and then used as base metals for bonding. The DB surfaces were prepared with conventional metallographic technique to obtain a highly polished flat surface.

Table-1 The parameter settings to bond Ti-alloy with AISI 410.

Specimen name	Process parameters °C/MPa/Min.	Shear strength MPa
S1	800,8, 45	16.4
S2	850,8, 45	52.6
S3	900,8, 45	64.2

The DB equipment consists of a hydraulic press with a built-in vacuum furnace and an inert gas purging facility. The test specimens were prepared with wire-cut electric discharge machining (WEDM) technique to obtain 4×40 mm diameter cylinders and 4×4×40 mm square section specimens. Conventional metallographic specimen preparation method was adopted for Vickers hardness, optical and scanning electron microscopy. This involves polishing the surface by applying silicon carbide paper starting from grit size 220 to 1200. Finally, the specimens were disc polished with an aluminium oxide slurry. The particle size of the slurry was varied from 1 µm to 0.25 µm to obtain a highly mirror finished surface.

3. RESULTS AND DISCUSSIONS

3.1. OPTICAL MICROSCOPY

The optical micrograph in Fig. 1 (a) shows a dark line at the interface indicating lack of diffusion between the two base metals. Atomic diffusion is noted at the interface; still it is not adequate to form a sound joint without defects because the processing temperature is only 800 °C. The thickness of the interface is controlled by bonding temperature alone because other parameters such as bonding time and holding pressure are constant for all the samples. The Fig. 1 (b) and (c) reveals a sound joint formation without defects at the interface. The samples S2 and S3 processed at 850 and 900 °C shows a thick interface with atomic diffusion of Ti, V, and Al into steel and Fe, Cr and C from AISI 410 steel side to Ti-alloy. The thickness of the diffused region is affected by three important parameters temperature, bonding time and heating rate. Further, a slow heating rate increases width of the reaction zone at higher temperatures.

The wavy interface in the Fig. 1 indicates breaking of surface irregularities and occurrence of plastic deformation prior to diffusion bonding. This technique prevents the formation of voids at the interface after bonding, further; this ensures uniform atomic diffusion from one base metal to another. This is in agreement with the observations made by Vigraman et al [8]. The atomic diffusion of Ti, Fe, Cr, Si, Mo and C resulted in the formation of intermetallic compounds and carbides such as Fe_2Ti, Ti_2Al, $FeAl_2$, Fe_3MnSi, TiAl, TiFe, FeSi, FeCrAl, CrC, VC and, TiC at the interface. The EDAX and XRD reports corroborate diffusion of various elements and formation of intermetallic compounds.

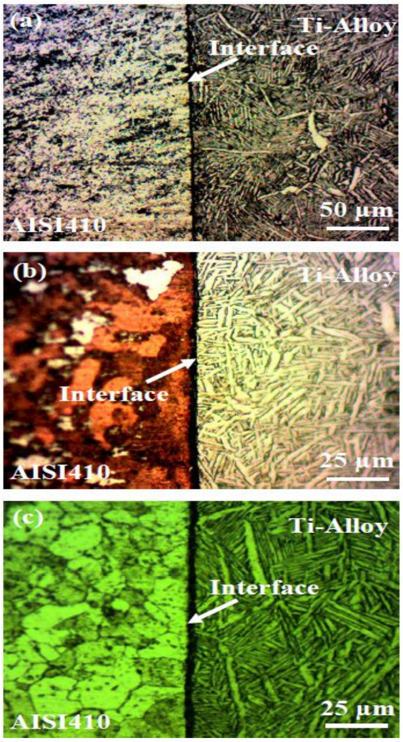

Figure 1: Optical micrographs (a) S1 bonded at 800 °C, (b) S2 bonded at 850 °C and (c) bonded at 900 °C.

3.2. SEM MICROGRAPHS

A SEM micrograph of the DB sample S1 is shown in Fig. 2 (a) and (b). In the microstructure shown in Fig. 2 (a), the bond zone indicates that it contains two small regions: a dark region near the stainless steel side and a region whitish in colour near the Ti-alloy side. Further, a dark straight line appears as a crack is noted at the interface between the base metals Ti-alloy and AISI 410 steel. The white fragmented phases seen throughout the Ti-alloy side are identified as 'β' (beta) phase which is in accordance with the observations made by Kundu et al [9]. In this Ti-alloy the amount of 'β' phase is more because it contains more amounts of 'β' stabilizing elements such as 'V', 'Mo' and 'Fe'. The dark matrix is 'α' (alpha) phase which is a solid solution of 'Ti' and 'Al'.

The thickness of the reaction zone has increased with increase in bonding temperature. The different phase mixtures at the interface of the parent metals are seen in the form of islands extending on both sides of the two base metals. The light and dark shaded regions on both sides of the interface represent solid solutions and intermetallic compounds formed because of diffusion of various elements across the interface. In the Fig. 2 (c) and (d) a homogeneous and a well diffused region at the interface close to the base metals is seen. On the right side of the micrograph at the AISI 410 side a short dark discontinuous line is seen which indicates the presence of a crack like defect. At the interface at one or two places dark points are seen indicating the presence of voids. Zang et al [10] reported the presence of voids at the interface of the DB joints.

The thickness of the reaction zone has increased with increase in bonding temperature in comparison with the micrograph shown in Fig. 2 (a). The different phase mixtures at the interface of the parent metals are seen in the form of islands extending on both sides of the two base metals. The light and dark shaded regions on both sides of the interface represent solid solutions and intermetallic compounds formed because of diffusion of various elements across the interface. In these regions more pronounced diffusion of alloying elements such as Ti, Al, V, Fe, Cr, and C has taken place from concentration rich regions to concentration less regions. As depth of diffusion increases the diffused elements reacts with the elements present in the alloy and forms intermetallic compounds. On the Ti-alloy side compounds such as Fe_2Ti, $FeAl_2$, TiAl, TiFe, FeCrAl, VC and TiC are formed. Similarly, at the AISI 410 steel side the intermetallic compounds such as Fe_2Ti, $FeAl_2$, TiAl, Fe_3MoSi, TiFe, $MoSi_2$, FeCrAl, CrC, VC and, TiC are formed. The presence of the 'β' phase, FeTi and Fe_2Ti closer to the interface is confirmed by the reported work of Kundu et al [11].

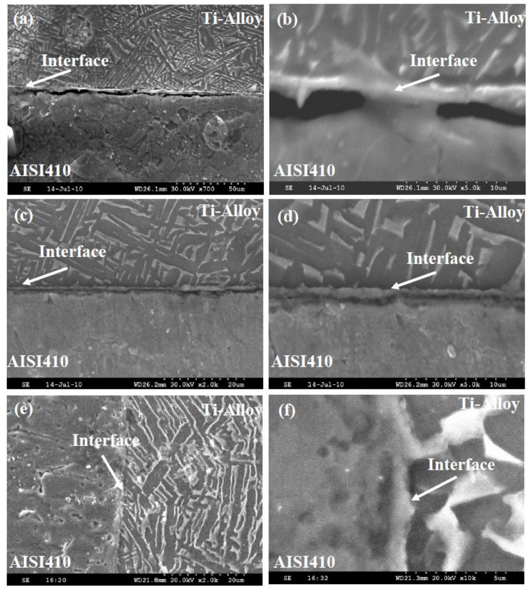

Figure 2: SEM micrographs (a) and (b) S1 bonded at 800 °C, (c) and (d) S2 bonded at 850 °C and (e) and (f) bonded at 900 °C.

Titanium aluminides form closer to the interface in the Ti-alloy and at the interface because of the migration of 'Al' atoms towards the AISI 410. As the 'Al' concentration increases beyond 5.5% at the interface, the formation of such compounds occurs. This observation is in good agreement with the observations made in the ASM Handbook by Gammon et al [12]. At the interface, intermetallic compounds such as Fe_2Ti, $FeAl_2$, TiAl, Fe_3MoSi, TiFe, $MoSi_2$, FeCrAl, CrC, VC and, TiC are noted. The presence of these compounds is confirmed by the XRD analyses performed on that region and given in Table 2

Table-2 The intermetallic compounds formed in the DB samples.

Type of compounds formed	Sample Number			Crystal structure
	S1	S2	S3	
	Weight percentage compounds			
410 steel	63.4	59.5	60	Cubic
Al	5.6	4.1	4.2	Cubic
Fe_3Al	2.8	3.2	3.5	Cubic
TiAl	1.8	2.6	1.8	Hexagonal
Fe_3MoSi	5.2	3.8	3.8	Cubic
FeTi	1.2	1.6	1.8	Cubic
TiSi	1.8	1.6	1.6	Orthorhombic
CrC	0.8	1.2	1.2	Cubic
TiC	1.8	3.4	3.4	Cubic
VC	1.4	2.2	2.1	Cubic
$VCrFe_8$	2.4	4.3	4.5	Cubic
Fe_4V	1.1	1.8	1.8	Cubic
FeCrAl	2.8	2.8	2.1	Cubic
Fe_2VAl	2	2	2	Cubic
$MoSi_2$	2	2	2	Cubic
Ti_2Al	1.1	1.4	1.8	Cubic
$FeAl_2$	1.2	1.3	1.2	Cubic
$AlFe_2V$	1.6	1.2	1.2	Cubic
Total	100	100	100	

The width of the interfacial reaction zone increases as the bonding temperature increases from 800-900°C as seen in Fig. 2 (e) and (f). . In the AISI 410 side, martensite phase and fine carbides along with intermetallic compounds are noted. At the Ti-alloy side the presence of alpha and beta phases are noted. Further, closer to the interface greyish colonies and dark shaded islands are seen along with whitish beta phase. From the EDAX report it is understood that the diffusion of Ti to the AISI 410 side is faster than diffusion of Fe to the Ti alloy side because of this interface migration takes place. An indistinguishable interface is formed between the Ti-alloy and AISI 410 steel. Aleman et al [13] reported that this was like Kirkendall effect. At higher temperatures, small pin like voids are formed because of the driving force of thermal energy supplied to the DB couple. In general, atoms migrate from higher concentration to lower concentration regions during DB process. These vacancies are created during DB that leads to the formation of voids due to thermodynamic non-equilibrium conditions that exists closer to the interface. The thermodynamic non-equilibrium conditions are created because of difference in diffusivity existing between various elements which results in creation of voids as reported by Srikrishnan et al [14].

By increasing the bonding temperature 'Fe' and 'Cr' diffused from the base metal AISI 410 steel to the Ti-alloy. Diffusivity increases with respect to rise in temperature for various alloying elements present in the alloy systems, according to the Arrhenius equation.

The diffusivity is measured after measuring the concentration of an element (C_x) at a distance 'x' from the interface, the Fick's second law is rewritten as given below.

$$\frac{\partial C_x}{\partial t} = D\left(\frac{\partial^2 C_x}{\partial x^2}\right) \quad (1)$$

The solution to this equation is as follows:

$$C(x,t) = A - B\,erf\left(\frac{x}{2\sqrt{Dt}}\right) \quad (2)$$

$$A = \left(\frac{C_1 + C_2}{2}\right),\ B = \left(\frac{C_2 - C_1}{2}\right) \quad (3)$$

where C_1 and C_2 are the initial concentrations of the element under study in both sides of the diffusion couple, 'x' is the distance from the interface, 't' is the bonding time and 'D' is diffusion coefficient as mentioned by Raghavan [15]. The diffusivity of various elements across the interface and formation of intermetallic compounds at the interface and at the base metals regions are confirmed in the published work of Wei Li et al [16].

3.3. MECHANICAL PROPERTIES

The shear strength of the DB sample S1 processed at 800 °C, yielded a minimum value of 16.4 MPa as given in Table 1. The reason for the poor shear strength is attributed to low mobility of diffusing atoms across the interface into the base metals. Maintaining higher temperatures provides the thermal energy required for activating the atoms to migrate from one point to another point. The shear strength of the DB joints was on the rise with increasing temperature. For the samples S2 the shear strength was 52.6 MPa and a maximum value of 64 was recorded for the sample S3 processed at 900 °C. The maximum shear strength 64.2 MPa itself, is a low value compared to the base metals shear strength. Longer holding time reduces shear strength of the DB joints because of grain growth and formation of intermetallic compounds and secondary phases which retards diffusion. Referring to the microstructures shown in Fig. 1 and 2 it is evident that a sound DB joints are formed. On the contrary to the evidence the shear strength of DB joints were low because of contamination of the interface during bonding. The reason could be failure of vacuum leading to the presence of oxides and formation of intermetallic compounds during bonding.

Vickers microhardness values were measured from the interface towards the base metals Ti-alloy and AISI 410 steel as shown in Fig. 3. At the interface the hardness value is 368.9 for the sample processed at 800 °C. The diffusion couples bonded at the lower bonding temperature have smaller hardness values. The reason is attributed to the small amount of intermetallics formed at the interface and at the adjacent regions of the base metal regions. At the interface the hardness value is only 428.7 for the sample processed at 900 °C. The hardness value is 405.2 at the interface for the sample S 2. In general a interface maximum hardness values were realized because of the formation of hard and brittle intermetallic compounds. The present study contradicts the observations made by Kundu et al [17]. The decrease in hardness value is because of presence of cracks and voids in the joints. The hardness values were maximum at the region closer to the interface than at the interface. On the Ti-alloy side the Vicker's hardness values were more than the base metal AISI 410 steel side.

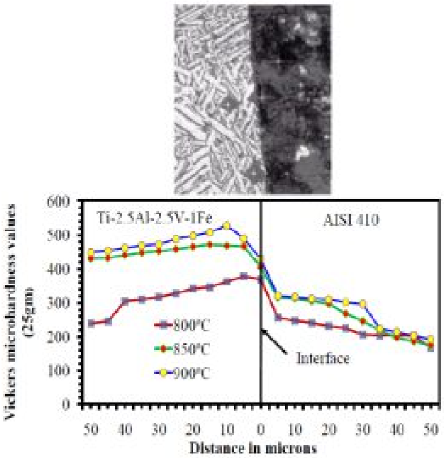

Figure 3: The Vickers microhardness profile of the DB samples.

A maximum hardness value of 528.1 was recorded at a distance of 10 microns from the interface towards the base metal Ti-alloy side for the sample S 3. On the stainless steel side a maximum hardness value of 320.6 is recorded for the sample processed at 900 °C. The microhardness values reported in the present study are confirmed in the published work of Araee and Sabetghadam [18]. The diffusion of the main alloying elements in the interfacial regions is the key parameter while controlling the performance of the joints. The gradual change of hardness values across the interfaces indicates the formation of hard phases closer to the interface along the base metals. On the contrary Kundu et al [19] observed that the interface hardness values were higher than the base metal hardness values.

3.4 SEM FRACTOGRAPHY

The fractured surfaces of the shear test samples were examined with SEM. All of the shear test samples failed at the interface and exhibited a brittle mode of fracture. The hard and brittle intermetallic compounds formed at the interface and presence of cracks and voids could be the reason for the brittle failure. The fractographs shown in Fig. 4 (a) and (b) indicates the presence of few small dimples and large cleavages. This indicates the mode of fracture is brittle in nature.

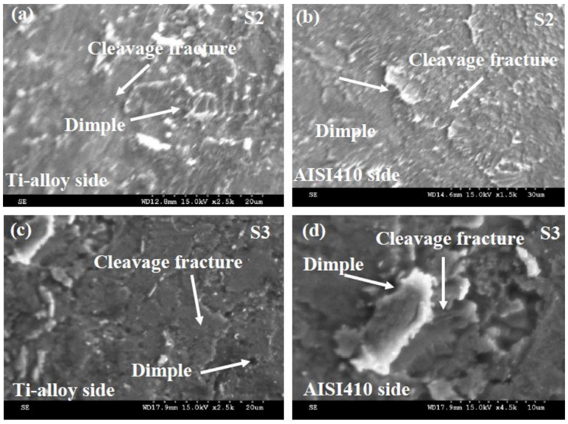

Figure 4: SEM fractographs: (a) S2, Ti-alloy side, (b) S2, AISI 410 side, (c) S3, Ti-alloy side and (d) S3, AISI 410 side.

During the shear test, the fracture took place at the interface between the Ti-alloy and AISI 410 steel. The cleavage pattern is an evidence of brittle fracture and low shear strength. In the Fig. 4 (c) and (d) very fine dimples and cleavages are seen. The amount of dimples present in the micrographs reveals the mode of fracture is brittle. The brittle fracture took place at the interface is in agreement with the observations made by Kundu et al [19].

4. CONCLUSIONS

The direct DB of Ti-4.5Al-2Mo-1.8V-0.5 Fe with AISI 410 was carried out and the following conclusions were arrived.

- Diffusion bonded samples processed at temperature 900 °C, bonding time 45 min and holding pressure 8 MPa yielded a maximum shear strength of 64.2 Mpa.

- The decrease in mechanical properties was attributed to the formation of intermetallic compounds at the interface..
- The EDAX reports indicated that the diffusivity of 'Ti is higher than 'Fe'.
- Maximum hardness value of 528.1 VHN was recorded for the DB samples processed at 900°C in the Ti-alloy base metal region. The increase in hardness was due to the formation of intermetallic compounds at higher temperatures.
- The XRD analysis confirmed the presence of Fe_2Ti, Ti_2Al, $FeAl_2$, Fe_3MoSi, TiAl, TiFe, $MoSi_2$, FeCrAl, CrC, VC and, TiC at the joint region.

REFERENCES

1. Sedat Kolukisa, (2007), "The effect of the welding temperature on the weldability in diffusion welding of martensitic (AISI 420) stainless steel with ductile (spheroidal graphite-nodular) cast iron", Journal of Materials Processing Technology, 186, 33–36.
2. Vigraman T, Narayanasamy R, and Ravindran D, (2012), "Microstructure and mechanical property evaluation of diffusion-bonded joints made between SAE 2205 steel and AISI 1035 steel", Mater. Design, 35, 156-159..
3. He P, Feng J C, Zhang B .G, and Qian Y. Y (2003), "A new technology for diffusion bonding intermetallic TiAl to steel with composite barrier layers", Materials Characterization, 50, 87– 92.
4. Kundu S and Chatterjee S, (2008), "Diffusion bonding between commercially pure titanium and micro-duplex stainless steel", Materials Science and Engineering A, 480, 316–322.
5. Kundu S and Chatterjee S, (2006), "Interfacial microstructure and mechanical properties of diffusion-bonded titanium–stainless steel joints using a nickel interlayer", Materials Science and Engineering A, 425, 107–113.
6. Qin B, Sheng G M, Huang J W, Zhou B, Qiu S Y and Li C, (2006), "Phase transformation diffusion bonding of titanium alloy with stainless steel", Materials Characterization, 56, 32–38.
7. Kundu S, Ghoshb M, Laik A, Bhanumurthy K, Kale G B and Chatterjee S, (2005), "Diffusion bonding of commercially pure titanium to 304 stainless steel using copper interlayer", Materials Science and Engineering A, 407, 154–160.
8. Vigraman T, Ravindran D and Narayanasamy R, (2012), "Effect of phase transformation and intermetallic compounds on the microstructure and tensile strength properties of the diffusion-bonded joints between Ti-6Al-4V and AISI 304L", Mater. Design, 36, 714-727.
9. Kundu S and Chatterjee S, (2006), "Interfacial microstructure and mechanical properties of diffusion bonded titanium-stainless steel joints using a nickel interlayer", Mater. Sci. Eng. A, 425, 107-113.
10. Zhang C, Li H and Li M.Q, (2015), "Formation mechanisms of high quality diffusion bonded martensitic stainless steel joints", Science and Technology of Welding & Joining, 20, 115-122.
11. Kundu S. and Chatterjee, S. (2008), "Diffusion bonding between commercially pure titanium and micro-duplex stainless steel", Mater. Sci. Eng .A, 480, 316-322.
12. Gammon L. M., Briggs, R. D., Packard, J. M., Batson, K. W. and Boyer, R., Domby, C. W. (2004), in: "Metallography and Microstructures of Titanium and Its Alloys, Metallography and Microstructures", ASM Handbook, ASM International, New York, Vol. 9, pp. 2157-2207.
13. Aleman, B., Guitierrez, I. and Urcola, J. J. (1993), "Interface microstructures in diffusion bonding of titanium alloys to stainless and low alloy steels", Mater. Sci. Technol, 9, 633-641.
14. Srikrishnan, V. and Ficalora, P. J, (1975), "Diffusion in transition metals and alloys", Metall. Mater. Trans. A, 6, 2095-2102.
15. Raghavan, V, (2004), "Mater. Sci. and Engg.", Prentice Hall India Ltd., New Delhi, 178-200.
16. Wei Li, Frank Liou, Joseph Newkirk, Karen M. Brown Taminger, and William J. Seufzer, (2017), "Ti6Al4V/SS316 multi-metallic structure fabricated by laser 3D printing and thermodynamic modeling prediction", Int J Adv Manuf Technol, 1-13.
17. Kundu, S. and Chatterjee, S, (2010), "Evolution of Interface Microstructure and Mechanical Properties of Titanium/304 Stainless Steel Diffusion Bonded Joint Using Nb Interlayer", ISIJ International, 50, 1460-1465.
18. Araee A and Sabetghadam H, (2010), "Characteristics of Diffusion Annealing Between Martensitic Stainless Steel and Nickel in the Form of Coating and Foil", Journal of Materials Engineering and Performance, 19, 1015–1021.
19. Kundu, S., Sam, S. and Chatterjee S, (2011), "Interface microstructure and strength properties of Ti-6Al-4V and microduplex stainless steel diffusion-bonded joints", Mater. Design, 32, 2997-3003.